第7卷 第3期 天 文 学 进 展 Vol. 7, No. 3
1989年7—9月 PROGRESS IN ASTRONOMY July—Sept., 1989

GAMMA RAYS FROM AGNs

E. C.M. Young and K.N. Yu

(Department of Applied Science, City Polytechnic of Hong Kong)

Abstract

In the first part of this paper, we have described the identification of γ-ray AGNs by using the database of cosmic γ-rays above 100 MeV from the SAS-2 satellite. Gamma-ray emissions from 11 quasars, 3 BL Lac Objects and 1 radiogalaxy have been identified.

In the second part of this paper, we have described the determination of the contribution from AGNs to the extragalactic γ-ray background. The SAS-2 γ-ray data have been employed to determine the functional relationships between the absolute γ-ray luminosities $L\gamma$ and the absolute optical luminosities of quasars and Seyfert galaxies. From these, their contribution to the extragalactic γ-ray background have been derived. We have shown that quasars ($B<20$) and Seyfert (Type 1 and 1.5) galaxies together contribute to a substantial part (about 59%) of the diffuse γ-ray background in the 35—100 MeV range. We conclude that the extragalactic γ-ray background is likely to be generated by active galaxies such as quasars and Seyfert galaxies.

In the third part of this paper, we have combined the data from the γ-ray region and those from other wavebands for 3 γ-ray AGNs to investigate the emission mechanisms of radiations from these objects. These gamma ray data together with data in other wavebands give severe constraints to the emission mechanisms of radiations from these objects. We have shown that the data for these three objects agree with those predicted by the synchrotron self-Compton (SSC) model.

1. INTRODUCTION

The γ-ray data from AGNs are important in that these can be used to give clues to the emission mechanisms of radiation from these objects, and to the origin of the extragalactic γ-ray background. There are three parts in this paper, namely the identifications of γ-ray AGNs, the determination of the contribution from γ-ray AGNs to the extragalactic γ-ray background, and the investigation of a possible emission mechanism for the radiation of the AGNs in view of the new data.

In the first part, we attempt to search for extragalactic γ-ray sources using

Received January 9, 1989.

the cosmic γ-ray database [1] from the SAS-2 whole sky survey. Although the COS-B data were used in detecting γ-rays from some of the extragalactic sources such as the Perseus Cluster[2] and the quasar 3C273[3,4], the high and somewhat uncertain instrumental background of the COS-B detector precludes the search for γ-ray fluxes from fainter sources. Despite poor statistical precision, the SAS-2 instrumental background is very low so it seems appropriate to use the SAS-2 data to search for γ-ray fluxes from extragalactic objects.

As γ-ray signals can be detected from extragalactic objects such as the quasars[3-7], the Seyfert galaxy NGC4151[5] and radiogalaxies[5-7], it becomes apparent that there are contributions from these objects to the extragalactic γ-ray background. Their contributions have been considered previously[8-12]. However, their luminosity functions have not been made used of so the calculations are not very accurate. In the second part of this paper, we find the contributions from quasars and Seyfert galaxies as classes of objects to the diffuse γ-ray background in the range of 35—100 MeV by first establishing their luminosity functions in the corresponding energy range[13].

In the third part of this paper, we try to show that the new γ-ray data of the AGNs are consistent with the well-known SSC (Synchrotron self - Compton) model.

We choose the Hubble constant to be $H_0 = 50\ \mathrm{km \cdot s^{-1} \cdot Mpc^{-1}}$ and the deceleration parameter to be $q_0 = 0.5$ in all the calculations of this paper. The difference introduced by using other values of H_0 and q_0 will not be significant.

2. THE IDENTIFICATION OF GAMMA-RAY AGNs

2.1. The Correlation Analysis

In searching for γ-rays from discrete sources, one attempts to look for statistically significant excesses above the background at the positions of the discrete sources. The main limitation of the γ-ray date available today, e. g. those from the SAS-2 and COS-B satellites, is the small number of photons detected and the poor angular resolution of the detectors. As a result we have used the "cross-correlation" method devised by Hermsen[14] for the analysis of the raw γ-ray data.

With the cross-correlation method, the distribution of the photon arrival directions is correlated with the detector pointspread function (PSF). A structure in the raw data consistent with the PSF produces a maximum signal whereas other structures are suppressed.

A γ-ray source is then defined as a significant excess of the correlated count or the correlated flux over the underlying background. Therefore the most important information from cross-correlating the raw data for accepting or rejecting a point source as a γ-ray source is then correlated strength of the source expressed in the correlated counts C_n and the parent standard deviation of the underlying background σ_0. In the case of a source satisfying a preset detection criteria, the standard deviation of the source strength $\sigma(C_n)$ can also be derived. The expressions of these quantities are given by Hermsen[14]as,

$$C_n(r) = (m\Sigma fN - (\Sigma f)(\Sigma N)\frac{\Sigma f}{m\Sigma f^2 - (\Sigma f)^2}, \tag{1}$$

$$C_n/\sigma_0 = \frac{(m\Sigma fN - (\Sigma f)(\Sigma N))}{\{[m\Sigma f^2 - (\Sigma f)^2][\Sigma N]\}^{1/2}} \tag{2}$$

and

$$\sigma(C_n) = [\gamma\Sigma N]^{1/2} \tag{3}$$

with

$$\gamma = \frac{m^2\Sigma f^3 - 2m\Sigma f\Sigma f^2 + (\Sigma f)^3}{[m\Sigma f^2 - (\Sigma f)^2]^2}\Sigma f_0 \tag{4}$$

where $f(r,i,j)$ is the detector PSF and predicts the contribution of a source at r to bin (i,j), N_{ij} is the count value of the bin (i,j) and m is the number of bins over which $\sum_{ij}$ is accumulated. The value of $\sigma(C_f)$ is approximated by

$$\sigma(C_f) = \sigma(C_n)C_f/C_n, \tag{5}$$

where C_f is the correlated flux given by an expression similar to equation(1), which is written as,

$$C_f(r) = (m\Sigma fF - (\Sigma f)(\Sigma F))\frac{\Sigma f}{m\Sigma f^2 - (\Sigma f)^2}, \tag{6}$$

where F_{ij} is the flux value of the bin (ij).

2.2 The Search for γ-ray Sources

The PSF of a detector is expressed as[14]

$$f(\theta) = N\exp(-(\theta/\theta_0)^{2c}) \tag{7}$$

where N is a normalisation constant, θ is the angular distance from the source, θ_0 and c are parameters that are different for different detectors and received photon energies. We adopt the values[15] of $\theta_0 = 1°.52$ and $c = 0.5$ for $E_\gamma > 100$ MeV, and $\theta_0 = 5°$ and $c = 0.8$ for 35 MeV $< E_\gamma < 100$ MeV for the SAS-2 detector.

We exclude the region of the Galactic plane($|b| \leqslant 22°$) to avoid the influence of Galactic sources which will affect the values of correlations. We also exclude all the bins with $|b| > 73°.4$ since the SAS-2 bins are too large here to give good positional accuracies.

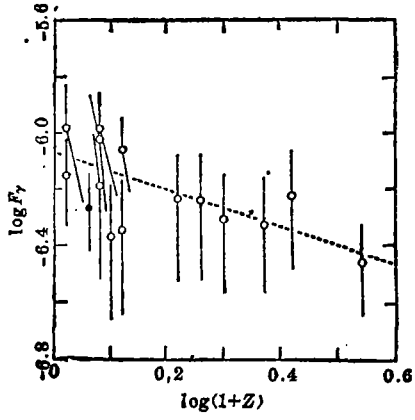

Figure 1 The distribution of log$F\gamma$(>100MeV) ($F\gamma$ in units of photons·s^{-1}·cm^{-2}) with the log (1+Z). The dotted line is the regression line(Eq. (8)). The point for the quasar 3C273 shown by a filled circle is included for comparison

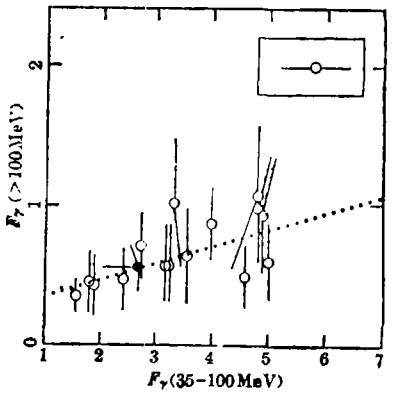

Figure 2 The distribution of $F\gamma$(>100 MeV) with $F\gamma$(35—100 MeV), both in units of 10^{-6} photons·s^{-1}·cm^{-2}. The uncertainties in Fγ (35—100 MeV) are omitted for the sake of clarity (a typical uncertainty is shown in the box in the upper right corner of the figure). The dotted line is the regression line(Eq. (9)). The point for the quasar 3 C273 shown by a filled circle is included for comparison

Table 1

The γ-ray fluxes and the γ-ray spectral indices of the 15 AGNs

(from Young and Yu[6])

Object	Type[a]	Z	$F\gamma$(>100 MeV) ($\times10^{-6}$photons·s^{-1}·cm^{-2})	$F\gamma$(35—100 MeV) ($\times10^{-6}$photons·s^{-1}·cm^{-2})	$a\gamma$
1144+115	Q	2.438	0.35±0.12	1.56±0.30	2.62(3.10,2.24)
1121+423	Q	0.234	0.43±0.21	1.88±0.34	2.60(3.29,2.17)
1238+006	Q	0.31	0.45±0.22	1.81±0.36	2.53(3.23,2.09)
1328−034	Q	1.352	0.47±0.22	2.41±0.36	2.73(3.37,2.31)
1011+250	Q	1.631	0.60±0.27	4.99±0.65	3.13(3.75,2.70)
1352−104	Q	0.332	0.87±0.26	3.98±0.44	2.63(3.01,2.35)
0923+201	Q	0.190	0.94±0.42	4.88±0.68	2.74(3.34,2.34)
1800+440	Q	0.663	0.57±0.27	2.70±0.58	2.67(3.36,2.21)
1806+456	Q	0.830	0.57±0 27	2.70±0.58	2.67(3.36,2.21)
0251−675	Q	1.002	0.49±0.22	4.58±0.63	3.23(3.84,2.79)
0153−520	Q	0.19	0.64±0.34	3.55±0.91	2.79(3.63,2.24)
1133+704	B	0.046	1.02±0.46	3.31±0.82	2.38(3.02,1.94)
0317+185	B	0.19	0.98±0.38	4.80±1.08	2.69(3.27,2.26)
0306+102	B	.....	1.07±0.50	4.80±1.08	2.62(3.31,2.16)
1130−037	R	0.0482	0.71±0.24	2.73±0.35	2.50(2.93,2.19)

a Q: quasars; B: BL Lac objects; R: radiogalaxy

2.3. The Gamma Ray AGNs

The criteria for accepting a γ-ray excess as a genuine γ-ray source has been derived by Young and Yu[6]. In the region $22° < |b| \leqslant 73°.4$, there are 15 AGNs which have satisfied the preset criteria. In Table I, we have listed the redshifts, the γ-ray fluxes for the two energy ranges $F_\gamma(>100$ MeV) and $F_\gamma(35—100$ MeV), and the derived γ-ray spectral indices α_γ for the 15 AGNs. In Figure 1, we have plotted the distribution of $F_\gamma(>100$ MeV) (in units of 10^{-6}— photons$\cdot s^{-1}\cdot cm^{-2}$) with the redshift z, which can be expressed as

$$\log F_\gamma(>100 \text{ MeV}) = -(6.07\pm0.08) - (0.66\pm0.31)\log(1+z) \qquad (8)$$

with a correlation coefficient $\rho_1 = -0.74$. It is therefore seen that in general F_γ decreases with z. The presence of a good correlation rules out the possibility that the γ-ray fluxes come from random fluctuations. In Figure 2, we show the relationship between $F_\gamma(>100$ MeV) and $F_\gamma(35$–100 MeV), which can be expressed as

$$F_\gamma(>100 \text{ MeV}) = (0.12\pm0.05)\times F_\gamma(35—100 \text{ MeV}) + (0.22\pm0.15)\times 10^{-6} \qquad (9)$$

with a correlation coefficient $\rho_2 = 0.71$. The good correlation and the positive slope are expected for genuine extragalactic sources. From equation (9), we can see that the regression line does not pass through the origin, which may be explained by the selection effect, i.e. the smaller values of F_γ (>100 MeV) which should have been mostly found at low values of $F_\gamma(35—100$ MeV) are not detected as a result of the detector threshold.

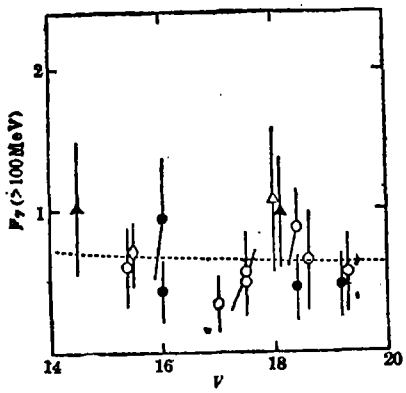

Figure 3 The distribution of $F\gamma$ (>100 MeV), in units of 10^{-6} photons$\cdot s^{-1}\cdot cm^{-2}$, with the V magnitudes of the AGNs. Circles: Quasars; Triangles: BL Lac objects; Rhombus: Radio galaxy; Filled symbols: V magnitudes detected with great accuracy; Outlined symbols: V magnitudes detected with great uncertainties (see text). The dotted line is the regression line (Eq. (10)).

2.4. Other Properties of the γ-ray AGNs

We then proceed to investigate the relationship between $F_\gamma(>100$ MeV) and the V magnitudes and the flux values F_X at 2 keV of the AGNs, and the relationship

between the γ-ray luminosities and the optical luminosities of the AGNs.

In Table II, we have listed the V magnitudes, redshifts and the vaues of F_γ (> 100 MeV)for the 15 AGNs. The distribution of F_γ (>100 MeV) with the V magnitudes of the AGNs has been shown in Figure 3, the regression line of which is given by

$$\log F_\gamma(>100\text{MeV}) = (-5.68\pm1.73) - (0.41\pm1.40)\log V \qquad (10)$$

with a correlation coefficient of -0.10. Therefore the correlation between F_γ (> 100 MeV) and V is poor. This may be attributed to several reasons. One of them is the large uncertainties in some of the V magnitudes which may be 0.5—1.0 magnitudes (Hewitt and Burbidge, 1980) and these are shown by outlined symbols in Figure 3. The other reason is that the V magnitudes are not corrected due to strong emission lines and Galactic absorption. These effects are reflected by the correlation coefficient between log V and $\log(1+z)$ for our sample which is only 0.20. The correlation between F_γ (>100 MeV) and V is worsened by the variability of the AGNs in both wavebands and the non-simultaneous detections of the sources. As the uncertainties introduced by those in the V magnitudes and the variabilities of the AGNs have overwhelmed that introduced by ignoring the corrections of the V magnitudes due to strong emission lines and Galactic absorption, these corrections have not been carried out. However, from Equation (10), we see that F_γ(>100 MeV) in general decreases with increasing V, i.e. the optically brighter objects are also brighter in γ-rays, which is expected.

There are altogether 6 AGNs in our sample that have X-ray data. We have calculated their X-ray fluxes F_X at 2 keV and these are listed in Table Ⅲ. The distribution of log F_γ (>100 MeV) with log F_X (2 keV) is shown in Figure 4, which can be expressed as

$$\log F_\gamma(>100\text{MeV}) = -(2.79\pm3.49) + (0.11\pm0.12)\log F_X(2\text{keV}) \qquad (11)$$

with a correlation coefficient of 0.56. A positive correlation between F_γ (>100 MeV) and F_X (2 keV)is shown, which implies that the objects brighter in X-rays are in general also brighter in γ-rays, which is again expected.

The optical luminosities L_O(in ergs·s^{-1}·Hz^{-1}) at 2500 Å and the γ-ray luminosities L_γ(in photons·s^{-1})>100 MeV are calculated respectively by using the following equations:

$$\log L_O = -0.4V - 0.5\ \log(1+z) + 2\ \log A(z) + 38.04 \qquad (12)$$

and

$$\log L_\gamma = \log F_\gamma - (1+\alpha_\gamma)\log(1+z) + 2\ \log A(z) + 57.63 \qquad (13)$$

where V are the V magnitudes of the AGNs given in Table Ⅱ, α_γ is the γ-ray spectral index taken from Bignami et al.[12] and Table 1 of the present paper which is

Table II

Object	V^a	z^a	$F\gamma(>100\text{MeV})$ $\times(10^{-6}\text{photons}\cdot\text{s}^{-1}\cdot\text{cm}^{-2})$
1144+115	.....	2.438	0.35±0.12
1121+423	16.02	0.234	0.43±0.21
1238+006	18.41	0.31	0.45±0.22
1328−034	19.18	1.352	0.47±0.22
1011+250	15.4	1.631	0.60±0.27
1352−104	18.4	0.332	0.87±0.26
0923+201	16.04	0.190	0.96±0.42
1800+440	17.5	0.663	0.57±0.27
1806+456	19.3	0.830	0.57±0.27
0251−675	17.5	1.002	0.49±0.22
0153−520	18.6	0.19	0.64±0.34
1133+704	14.49	0.046[b]	1.02±0.46
0317+185	18.12	0.19[c]	0.98±0.38
0306+102	18	.....	1.07±0.50
1130−037	15.50[d]	0.0482[d]	0.71±0.24

[a]From Hewitt and Burbidge[34] unless otherwise stated.
[b]From Schwartz and Ku[35].
[c]From Gioia et al[38].
[d]From Burbidge and Crowne[37].

Table III

Object		$\log[F_X(2\text{keV})]/\text{erg}\cdot\text{s}^{-1}\cdot\text{cm}^{-2}\cdot\text{Hz}^{-1}]$	Ref.
1101+250	QSO	−29.84	38
0923+201	QSO	−29.63	39
1806+201	QSO	−29.90	28
1133+704	BL Lac	−30.73	35
0317+185	BL Lac	−28.99	36
0306+102	BL Lac	−30.15	40

Table IV

Object	$\log L_o(2500\text{Å})$ $(\text{ergs}\cdot\text{s}^{-1}\cdot\text{Hz}^{-1})$	$\log L_\gamma(>100\text{MeV})$ $(\text{photons}\cdot\text{s}^{-1})$
1144+115	31.97	53.09(+0.13, −0.18)
1121+423	30.37	50.20(+0.17, −0.29)
1238+006	29.66	50.52(+0.17, −0.29)
1328−034	30.61	52.36(+0.17, −0.27)
1011+250	32.28	52.73(+0.16, −0.26)
1352−104	29.72	50.88(+0.11, −0.15)
0923+201	30.18	50.33(+0.16, −0.25)
1800+440	30.68	51.51(+0.17, −0.28)
1806+456	30.15	51.79(+0.17, −0.28)
0251−675	31.03	51.97(+0.16, −0.26)
0153−520	29.16	50.16(+0.19, −0.33)
1133+704	29.57	49.01(+0.16, −0.26)
0317+185	29.35	50.34(+0.14, −0.21)
0306+102	.....	.....
1130−037	29.21	48.89(+0.13, −0.18)

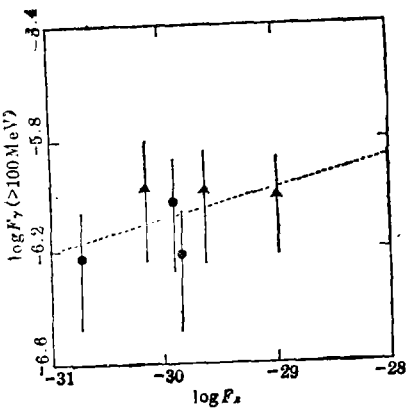

Figure 4 The distribution of log $F\gamma(>100$ MeV), in units of photons $\cdot s^{-1} \cdot cm^{-2}$, with $\log F_X$ (2 keV), in units of ergs $\cdot s^{-1} \cdot cm^{-2} \cdot Hz^{-1}$ of the AGNs. Circles: Quasars; Triangles: BL Lac objects. The dotted line is the regression line(Eq. (11))

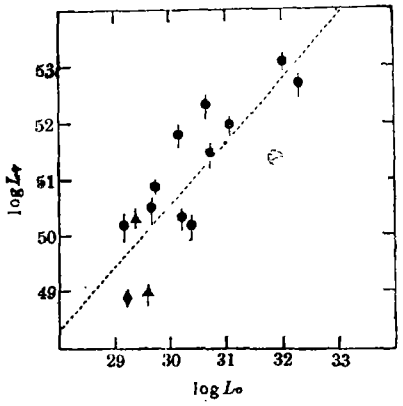

Figure 5 The distribution of $\log L\gamma(>100$ MeV), in units of photons $\cdot s^{-1}$, with $\log L_o$ (2500 Å), in units of ergs $\cdot s^{-1} \cdot Hz^{-1}$ of the AGNs. Circles: Quasars; Triangles: BL Lac objects. Rhombus: Radiogalaxy. The dotted line is the regression line (Eq. (14))

taken to be -2.7, and $A(Z)$ is the bolometric luminosity distance which is equal to $2\{(1+z)-\sqrt{1+z}\}$ for $q_0=0.5$. The values of L_O and L_γ are shown in Table Ⅳ.

The distribution of log L_γ with log L_O is shown in Figure 5, which can be expressed as

$$\log L_\gamma = (16.93\pm1.28) + (1.12\pm0.04)\log L_O \qquad (14)$$

with a correlation coefficient of 0.86. There is thus good correlation as expected. However, we see that L_γ is more than proportional to L_O, a result which seems to contradict to those in the X-rays and those obtained in the second part of this paper, which shows that both the X-ray and γ-ray luminosities are less than proportional to L_O. However, as our sample lacks low γ-ray flux objects, the objects detected with high optical luminosities which are mostly found at large distance are biased towards the brightest ones in γ-rays. Therefore the slope of the dependence of L_γ on L_O is steeper than the true one due to the selection effect.

2.5. Gamma Rays from Seyfert Galaxies

In the above, we can see that there are no Seyfert galaxies identified to be emitting >100 MeV γ-rays. This may be due to the small number of Seyfert galaxies used for analysis. Recently, Young and Yu[16] have searched for γ-ray AGNs outside the region $22°<|b|\leqslant73°.4$ and have confirmed >100 MeV from the three Seyfert galaxies NGC 4151, MCG 8-11-11 and 3 C120. Therefore it seems to us that Seyfert galaxies in general are also γ-ray emitters.

2.6. SAS-2 Results vs COS-B Results

The well known quasar 3C273 has previously been detected in γ-rays by using data from the COS-B[3,4]. During the analysis of the SAS-2>100 MeV γ-ray data, we[6]have identified γ-rays from the quasar with the probability of random detection being less than 8×10^{-5}. The flux value is found to be$(0.54\pm0.16)\times10^{-6}$ photons$\cdot s^{-1}\cdot cm^{-2}$, which is consistent with previous results. An upper limit of the flux of the quasar in the 35—100 MeV range has been determined to be $<2.68\times10^{-6}$ photons$\cdot s^{-1}\cdot cm^{-2}$. The data for 3C273 are also shown in Figures 1 and 2 for comparison and we see that agreement is apparent. The γ-ray spectral index is derived to be <2.99 which is also consistent with previous results.

The unidentified source 2CG 010-31 was found by the COS-B group[14] using the correlation function to have a γ-ray flux($E_\gamma>100$ MeV) of 1.2×10^{-6} photons$\cdot s^{-1}\cdot cm^{-1}$. It has been found[17] that the COS-B source may be related to an excess ($E_\gamma>100$ MeV) in the SAS-2 correlated data with the probability that the detection is due to random fluctuation being less than 10^{-5}. The γ-ray flux is $(1.17\pm0.27)\times10^{-6}$ photons$\cdot s^{-1}\cdot cm^{-1}$ which is in good agreement with that derived by Hermsen[14] using the COS-B data. However, the source for the γ-radiation remains unidentified.

Five of the 2CG sources of Hermsen[14] have also been identified (in a way that they satisfy the predetermined criteria) using the SAS-2 data[15]. The flux values derived are also in agreement with those derived by Hermsen[14]. The flux values from both the SAS-2 and COS-B experiments, for these five Galactic sources, together with those of the two high latitude sources described above, are shown in Figure 6. A very good agreement is apparent, and this shows again that it is consistently appropriate to apply the cross-correlation function method to the SAS-2 data.

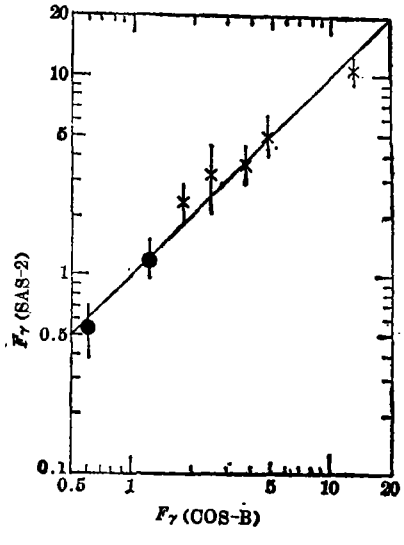

Figure 6 Comparison of the fluxes recorded by SAS-2 and COS-B for the 5 identified Galactic sources (shown by crosses) and for the two high latitude sources (shown by filled circles)

3. THE CONTRIBUTION FROM AGNs TO THE EXTRAGALACTIC GAMMA RAY BACKGROUND

3.1. The γ-ray Luminosity Functions

To calculate the contribution of different classes of discrete objects to the extragalactic γ-ray background, we need their γ-ray luminosity functions. Direct derivations of γ-ray luminosity functions should be based on complete samples in γ-rays of the corresponding classes of objects. However, up to now, only very few objects have been detected in γ-rays and no complete samples of objects in γ-ray have been obtained. Therefore the γ-ray luminosity functions can only be derived indirectly. We have to rely on luminosity functions in some other wavebands (e. g. the optical waveband at 2500 Å) where extensive investigations of the objects have been carried out, complete samples have been obtained and luminosity functions have been derived. We then proceed to find out the functional relationship between the absolute luminosities of these objects in that waveband and those in the 35—100 MeV range (L_γ, in photons·s^{-1}).

3.2. The Functional Relationship between the γ-ray Luminosities and the Optical Luminosities and the Optical Luminosities

In order to derive the functional relationship between L_γ and the luminosites in that waveband for a class of objects, we need to obtain γ-ray luminosities from a considerably large sample of that class of objects. As mentioned before, up to now, only very few detections of γ-ray objects have been achieved. The method we use in the present work is an extension of the one first devised by Houston et al[18]. In this method, we do not intend to identify the exact γ-ray fluxes or luminosities for each individual

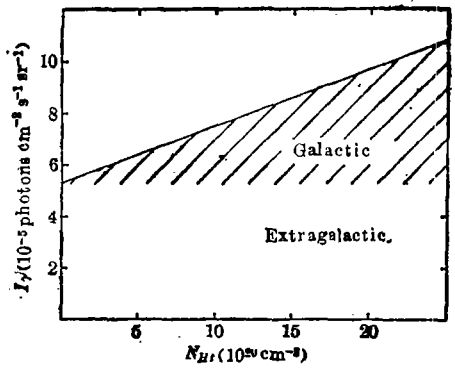

Figure 7 The relationship between the γ-ray intensities $I\gamma$ detected by SAS-2 and the total gas column densities N_{Ht} derived from Lick Survey galaxy count data is given by the solid line. The shaded part is the Galactic component which depends on the magnitude of the column density. The intercept is the extragalactic component

object. Instead we only determine their fluxes with respect to the average background. Some objects will fall above the average background and they are defined to be detections. Others will fall below the average background and the corresponding upper limits will be calculated.

The functional relationships between the absolute luminosities at 2500 Å (L_o, in ergs·s^{-1}·Hz^{-1}) and L_γ will be established. The "detections and bounds" (DB) method of Avni et al. [19] and the generalised regression analysis of Schmitt[20] will be used to cope with the upper limits of L_γ and to yield the required functional relationships, which are then combined with the luminosity functions for the classes of objects in the optical band to give the γ-ray luminosity functions. For quasars with B magnitudes <20, the optical luminosity function given by Marshall[21] is employed. For Seyfert galaxies of type 1 and 1.5, the optical luminosity function established by Cheng et al.[22] will be used.

3.3 The Galactic and Extragalactic Components of the Gamma Ray Background

We have to determine the expected Galactic matter contribution to the γ-ray flux along any direction from the cosmic ray-gas interactions, referred as the Galactic component. As data for total column density of gas (largely atomic and molecular hydrogen) are not available out of the Galactic plane where the extragalactic objects have been detected, we have to rely on the galaxy counts to estimate the total hydrogen column density N_{HT} of gas.

The method is similar to that first devised by Thompson and Fichtel[23]. The γ-ray intensities I_γ calculated from the SAS-2 data and the total hydrogen column densities N_{Ht} derived from the galaxy count data give an I_γ-N_{Ht} plot which is the solid lide[13] in Figure 7. The I_γ-N_{Ht} plot identifies the extragalactic component given by the intercept, as well as the Galactic component, the magnitude of which bears a linear relationship with the value of total hydrogen column density N_{Ht}.

3.4. The Statistical Detections and Upper Limits of Absolute Luminosities of Objects in the 35–100 MeV Range

We use AGN catalogues to search for γ-rays. Those "unusable" objects corresponding to no galaxy count data or insufficient (i.e., with an average value less than 15 units) SAS-2 telescope sensitivity are excluded from our analysis.

When the γ-ray intensity inthe direction of any remaining "usable" object exceeds the sum of the extragalactic component (i.e. the background radiation) and the corresponding Galactic component, i.e., when the object lies above the line in Figure 7, we define this net excess as a positive γ-ray detection from the object. When the usable objects do not have positive γ-ray detections, i.e., when they lie below the line in Figure 7, we calculate upper limits to their luminosities from the upper limits to their

fluxes determined from the corresponding SAS-2 sensitivity values and area factors.

We assume that the upper limits are drawn from the same sample as are the detections and that the γ-ray nondetections occur only because of the finite γ-ray flux threshold of the detector and not because there are other families of "γ-ray quiet" objects.

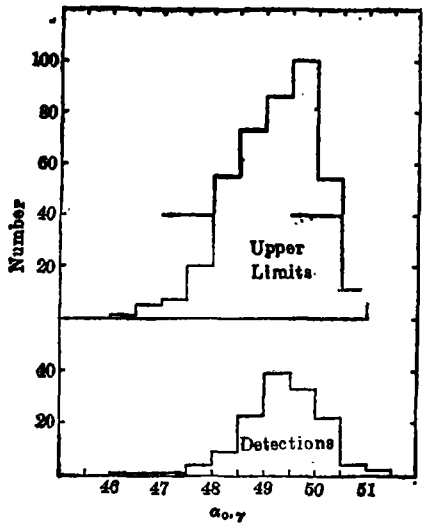

Figure 8 The distribution of $\alpha_{O,\gamma}$ for quasars. In the upper part, we have plotted the upper limits to $\alpha_{O,\gamma}$; in the lower part, the detections.

3.5. The Contribution from Quasars

We now proeed to determine the contribution from quasars to the extragalactic γ-ray background. We use the Hewitt and Burbidge[24]catalogue which contains 1491 quasars (excluding the 58 BL Lac Objects) to search for γ-ray flux from quasars. From the same catalogue, we also have the V magnitudes of the quasars. These can be used to derive the absolute optical luminosities L_O at 2500 Å (Eq•12).

In these 1491 quasars, there are 541 usable quasars, in which 129 are detections and 412 are upper limits, and these are shown graphically in Figure 8.

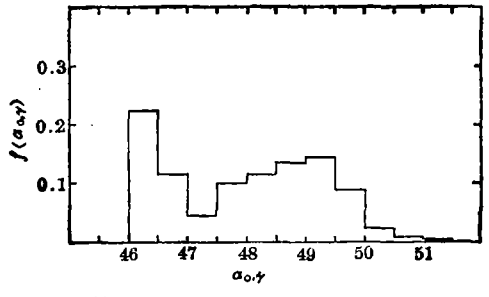

Figure 9 Differential $\alpha_{O,\gamma}$ distributions for quasars determined by the binned DB method

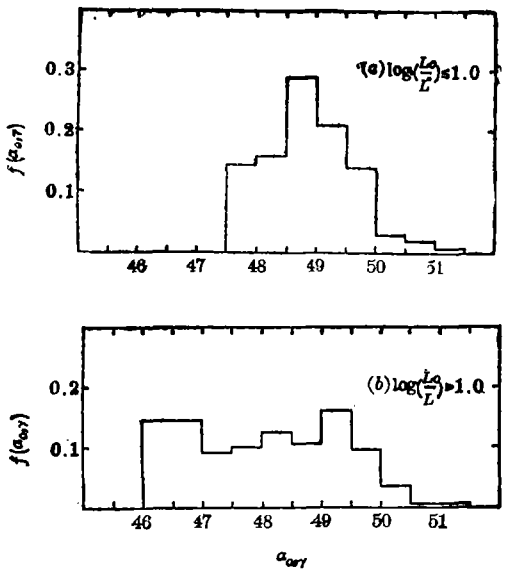

Figure 10 Differential α_{γ},γ distributions for (a) $\log(Lo/L^{*})\leqslant 1.0$ and (b) $\log(Lo/L^{*})>1.0$. The Kolmogorov-Smiruov(K-S)test statistic is much greater than the critical value at 98% confidence level. This implies that the two distributions are significantly different and that α_{O},γ should depend on $\log(Lo/L^{*})$

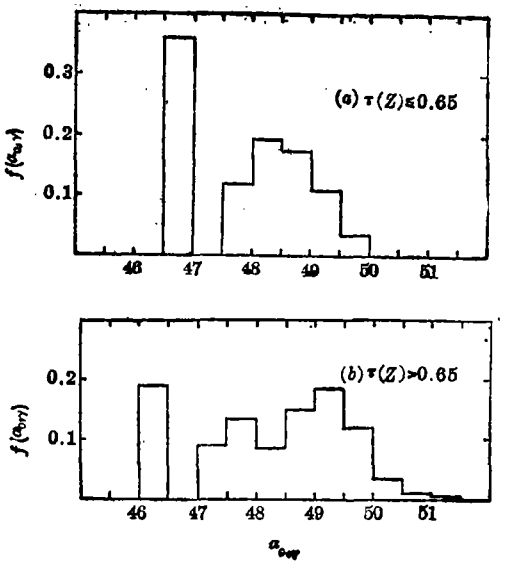

Figure 11 Differential α_{O},γ distributions for (a) $\tau(z)\leqslant 0.65$ and (b) $\tau(z)>0.65$. The Kolmogorov-Smirnov (K-S) test statistic is less than the critical value at 98% confidence level. This impiles that the two distributions are not significantly different and that α_{O},γ does not need to depend on $\tau(z)$

3.5.1. Dependence of γ-ray luminosity on optical luminosity and redshifts

We have defined a dimensionless parameter $\alpha_{O,\gamma}=\log(L_{\gamma}/L^{*})-\log(L_{O}/L^{*})$, which is similar to $\alpha_{O,X}$ being defined[19,25] as $\alpha_{O,X}=-\log(L_{X}/L_{O})/2.605$ where $L^{*}=1$ photon$\cdot s^{-1}$ and L_{X} (ergs$\cdot s^{-1}\cdot Hz^{-1}$) is the X-ray luminosity at 2 keV. In this case, upper limits to L_{γ} become upper limits to $\alpha_{O,\gamma}$. $L^{*}=10^{30}$erg $\cdot s^{-1}\cdot Hz^{-1}$.

In the calculations of the differential distributions of $\alpha_{O,\gamma}$, we have used both the detections and the upper limits of $\alpha_{O,\gamma}$ by using the DB method[19], which removes the selection effect that comes from the γ-ray flux threshold of the detector. The differential distributions of $\alpha_{O,\gamma}$ thus calculated are shown in Figure 9.

As quasars have large redshifts, we need to find the average dependence of $\alpha_{O,\gamma}$ of quasars on both the cosmological epoch and on optical luminosity, by checking the dependence of $\alpha_{O,\gamma}$ on the fractional look back time $\tau(z)$ $(=1-(1+z)^{-3/2}$ for $q_{O}=0.5)$ and on $\log(L_{O}/L^{*})$. To check any dependence of $\alpha_{O,\gamma}$ on $\log(L_{O}/L^{*})$ or $\tau(z)$, we divide our sample into two subsamples at certain values of $\log(L_{O}/L^{*})$ and $\tau(z)$ in turn and then compare the properties of the subsamples through the non-parametric Kolmogorov-Smirnov (K-S) test. These values are chosen to be $\log(L_{O}/L\ )=1$

and $\tau(z)=0.65$ (or $z=1$). The corresponding differential distributions of $\alpha_{O,\gamma}$ are shown in Figures 10 and 11 respectively. The test statistic in the $\tau(z)$ case is less than the critical value at 98% confidence level and this shows that the two distributions are not significantly different and that $\alpha_{O,\gamma}$ does not need to depend on the look back time. This recalls that the dependence of $\alpha_{O,X}$ on look back time has also been previously found to be weak and may be nonexistent[19,26], which suggests that the effect is intrinsic to physical processes that give rise to nonthermal emission in quasars. Since the production mechanisms of X-ray photons and γ-ray photons are somewhat similar, the result that $\alpha_{O,\gamma}$ also does not depend on the look back time is expected.

On the other hand, the test statistic in the $\log(L_O/L)$ case shows that the probability of no difference is 7.5×10^{-9}, so we can conclude that the two distributions are significantly different and that $\alpha_{O,\gamma}$ should depend on $\log(L_O/L)$. Also, it is highly unlikely for a randomly selected sample to have such significantly different subsamples, so we can also see that our sample does not come from random selections. We write

$$\alpha_{O,\gamma}=A\log\frac{L_O}{L}+B \tag{15}$$

where A and B are the regression coefficients. We use a generalised regression analysis[20] appropriate for this type of sample and obtain the results of

$$\alpha_{O,\gamma}=(-0.38\pm0.08)\log\left(\frac{L_O}{L}\right)+(49.50\pm0.13) \tag{16}$$

We can thus see that L_γ is less than proportional to (L_O/L) (or just L_O). The facts that $\alpha_{O,\gamma}$ depends on L_O and that L_γ is less than proportional to L_O immediately recall similar results in the X-ray case[26-28]. These point out the similarity between L_γ and L_X, and that the production mechanisms of X-ray photons and γ-ray photons in

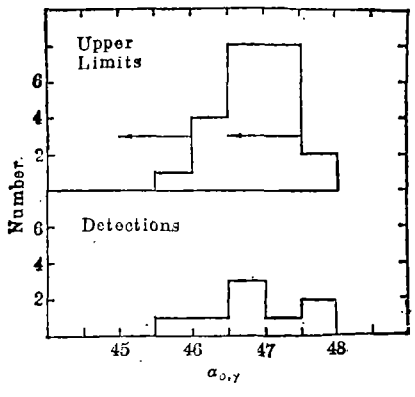

Figure 12 The distribution of $\alpha_{O,\gamma}$ for Seyfert galaxies (type 1 and type 1.5). In the upper part, we have plotted the upper limits to $\alpha_{O,\gamma}$; in the lower part, the detections

quasars might be somewhat similar, because both L_γ and L_X have a similar behaviour in the dependence on L_O.

3.5.2. The contribution from quasars

The cosmic intensity from quasars can be calculated from a cosmological integration. The pure luminosity evolution model[21] for quasars with B magnitudes<20, wherein their luminosities evolve as $(1+z)^{3.2}$ and the luminosity function is given by $dN/dL_O \propto L_O^{-3.8}$ has been adopted. We integrate to $z=3.5$. The cosmic intensity $I_{\gamma,O}$ contributed by quasars thus calculared is $(2.06^{+0.71}_{-0.53}) \times 10^{-5}$ photons $cm^{-2} \cdot s^{-1} \cdot sr^{-1}$.

Our own analysis[13] of the SAS-2 data gives the extragalactic component as $(5.3\pm0.7) \times 10^{-5}$ photons $cm^{-2} \cdot s^{-1} \cdot sr^{-1}$. It is therefore seen that quasars contribute $39^{+21}_{-13}\%$ to the diffuse γ-ray background in the 35—100 MeV range.

3.6. The Contribution from Seyfert Galaxies

For the Case of Seyfert galaxies, we have used the Seyfert galaxies (type 1 and type 1.5) that appear both in the Weedman catalogue[29,30] and in Cheng et al[22]. The reason for restricting the Seyfert galaxies to those in Cheng et al.[22] is that the nuclear magnitudes of those Seyfert galaxies are given. There are altogether 117 Seyfert galaxies.

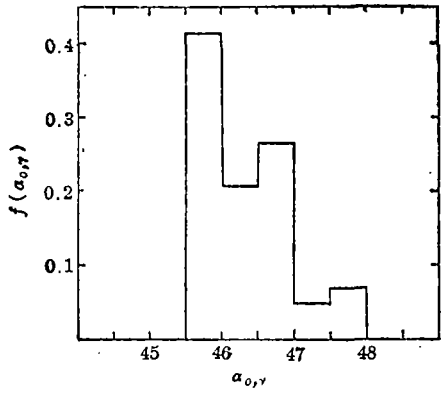

Figure 13 Differential $\alpha_{O,\gamma}$ distributions for Seyfert galaxies (type 1 and type 1.5) determined by the binned DB method

After deleting those with insufficient SAS-2 sensitivity and those with no galaxy count data, we are left with 30 Seyfert galaxies (type 1 and type 1.5) in which 8 are detections and 23 are upper limits. These are shown in Figure 12. The differential $\alpha_{O,\gamma}$ distributions calculated by using the DB method are shown in Figure 13. As Seyfert galaxies have small redshifts, we do not need to investigate the dependence of $\alpha_{O,\gamma}$ on z for Seyfert galaxies and we can assume no evolution for the luminosity function of Seyfert galaxies. Using the regression analysis given by Schmitt[20], we obtain the results of

$$\alpha_{O,\gamma} = (-0.21\pm0.45)\log\left(\frac{L_O}{L^*}\right) + (48.60\pm0.38) \qquad (17)$$

We can see again that L_γ is less than proportional to L_O. This shows that the emission mechanism of radiation in quasars and Seyfert galaxies are somewhat similar.

For computing the contributions $I_{\gamma,\,SG}$ from Seyfert galaxies to the diffuse γ-ray background in the 35—100 MeV range, we again make use of the cosmological integration equation. By using the luminosity function of Seyfert galaxies given by Cheng et al.[22], the cosmic intensity $I_{\gamma,\,SG}$ contributed by Seyfert galaxies has been calculated to be $(1.04^{+1.45}_{-0.81}) \times 10^{-5}$ photons $\cdot$ cm^{-2} $\cdot$ s^{-1} $\cdot$ sr^{-1}. We therefore see that Seyfert galaxies have a moderate contribution of $20^{+34}_{-13}\%$ to the diffuse γ-ray background in the 35—100 MeV range.

4. AN EMISSION MECHANISM FOR THE GAMMA-RAY AGNs

In this section, we have combined the data from the γ-ray region and those from other wavebands for 3 γ-ray AGNs, the quasars 1011+250 and 1352−104, and the BL Lac object 1133+704, to investigate the emission mechanisms of radiations from these objects. These gamma ray data together with data in other wavebands give

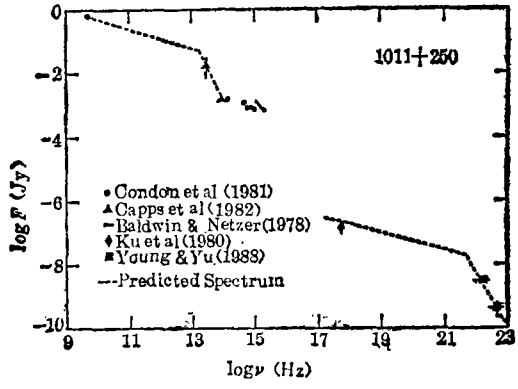

Figure 14　Spectrum of 1011+250

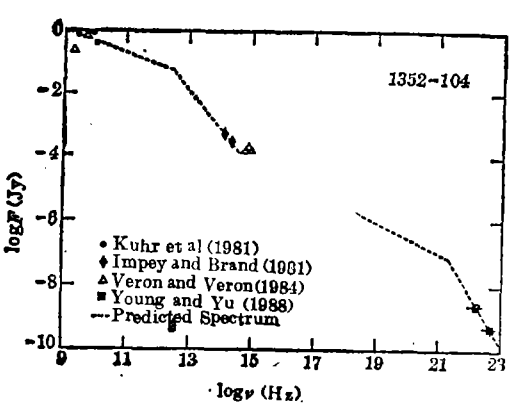

Figure 15　Spectrum of 1352−104

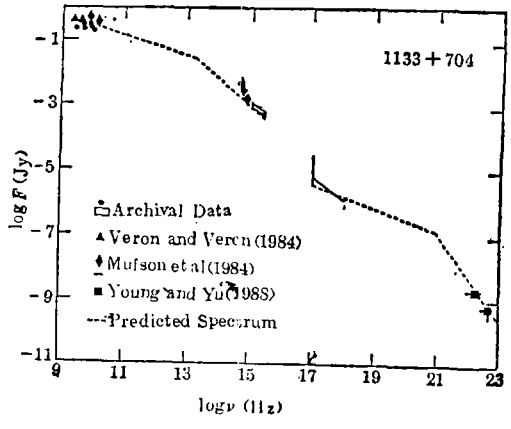

Figure 16　Spectrum of 1133+704

severe constraints to the emission mechanisms of radiations from these objects.

The models for the production of X-rays and γ-rays in AGNs include the jet model, the thermal bremsstrahlung model, the inverse Compton model and the most widely used synchrotron self-Compton (SSC) model. These models have been successfully applied in AGNs such as the BL Lac objects NGC1275 and Mrk501, the quasar 3C273, the Seyfert galaxies NGC4151 and MCG 8-11-11, and the radiogalaxy NGC 5128.[31] However, the existing data for the 3 objects allow a reasonably precise prediction only for the SSC model. We have therefore attempted to use this model to explain the observations.

The SSC model was proposed by Jones et al.[32] and it suggests that the X-ray and γ-ray photons from AGNs are generated from the inverse Compton scatterings of their own photons in the range from infrared to ultraviolet generated by synchrotron radiation. The predicted results from these 3 objects have been calculated[33] and shown in Figures 14 to 16. It can be seen that the data of the 3 objects studied can be very satisfactorily described by the SSC model and it has also been noticed that the γ-ray spectral indices of the objects agree with those predicted from the SSC model. It is here remarked that some of the data in the optical region of the spectra of the objects represents thermal emissions which cause an excess to the flux values in the region and these data should not be used for calculations. It should be clarified that we have shown that the SSC model is one of the models that can explain the data and we do not exclude other models, and the reason for investigating only the SSC model is solely that the existing data for the 3 objects only allow a reasonably precise prediction for the SSC model

5. DISCUSSIONS

In the first part of this paper, we have described the identification of γ-ray AGNs. The database of cosmic γ-rays above 100 MeV from the SAS-2 satellite has been analysed to identify γ-ray emissions from 11 quasars, 3 BL Lac objects and 1 radiogalaxy. Further investigations of their properties support that the sources detected are genuine extragalactic objects. The comparison between the results from the SAS-2 and the COS-B experiments shows that it is appropriate to apply the correlation analysis method to the SAS-2 data.

In the second part, we have described a method which allows us to obtain the functional relationships between the absolute γ-ray luminosities L_γ and the absolute optical luminosities of different classes of extragalactic objects such as quasars and Seyfert galaxies. From these, we are able to derive their contribution to the extraga-

lactic γ-ray background. We have shown that quasars ($B<20$) and Seyfert (Type 1 and 1.5) galaxies together contribute to a substantial part (about 59%) of the diffuse γ-ray background in the 35—100 MeV range. We can see that there is possible room for contributions from other classes of objects such as faint quasars (with $B\geqslant 20$), Seyfert (>1.5) galaxies, BL Lac objects, radio galaxies and normal galaxies. Considering the contributions from all these objects, we see that the total contributions from discrete extragalactic γ-ray sources to the diffuse background are likely to be very substantial, and may indeed account for nearly the entire background.

In the third part, we have combined the data from the γ-ray region and those from other wavebands for 3 γ-ray AGNs, the quasars 1011+250 and 1352−104, and the BL Lac object 1133+704, to investigate the emission mechanisms of radiations from these objects. These gamma ray data together with data in other wavebands give severe constraints to the emission mechanisms of radiations from these objects. The data of the 3 objects can be very satisfactorily described by the SSC model and it has also been noticed that the γ-ray spectral indices of the objects agree with those predicted from the SSC model. We have shown that the SSC model is one of the models that can explain the data.

Better understanding of the γ-ray properties of extragalactic objects and more accurate calculations may be achieved by using data from future γ-ray telescopes.

REFERENCES

[1] Fichtel, C. E., Hartman, R. C., Kniffen, D. A., Thompson, D. J., Ogelman, H. B., Tumer, T., and Ozel, M. E., *NASA Tech. Memo* 79650, (1978).

[2] Strong, A. W. and Bignami, G. F., *Astrophys. J.*, 274 (1983), 549.

[3] Swanenburg, B. N., Bennett, K., Bignami G. F., Caraveo, P., Hermsen, W., Kanbach, G., Masnou, J. L., Mayer-Hasselwander, H. A., Paul, J. A., Sacco, B., Scarsi, L., and Wills, R. D., *Nature*, **275** (1978) 298.

[4] Bignami, G. F., Bennett K., Buccheri, R., Caraveo, P. A., Hermsen, W., Kanbach, G., Lichti, G. G., Masnou, J. L., Mayer-Hasselwander, H. A., Paul. J. A., Sacco, B., Scarsi, L., Swanenburg, B. N., and Wills, R. D., *Astron. Astrophys.*, **93** (1981), 71.

[5] Houston, B. P. and Wolfendale, A. W., *Vistas in Astronomy*, **26** (1982), 107.

[6] Young, E. C. M. and Yu, K. N., *J. Phys. G.: Nucl. Phys.*, **14** (1988), L115.

[7] Young, E. C. M. and Yu, K. N., *Vistas in Astronomy*, **31** (1988), 579.

[8] Strong, A. W., Wolfendale, A. W., and Worrall, D. M., *J. Phys. A: Math. Gen.*, **9** (1976), 823.

[9] Bignami, G. F., Lichti, G. G., and Paul, J. A., *Astron. Astrophys.*, **68** (1978), L15.

[10] Schonfelder, V., *Nature*, **274** (1978), 344.

[11] Grindlay, J. E., *Nature*, **273** (1978), 211.

[12] Bignami, G. F., Fichtel, C. E., Hartman, R. C., and Thompson, D. J., *Astrophys. J.*, **232** (1979), 649.

[13] Young, E. C. M. and Yu, K. N., *Astrophys. J (Letters)*, **330** (1988), L5.

[14] Hermsen, W., Ph. D. Thesis, University of Leiden, (1980).

[15] Houston, B. P., Ph. D. Thesis, University of Durham, (1985).
[16] Young, E. C. M., and Yu, K. N., in preparation(1988).
[17] Yu, K. N., Ph. D. Thesis, University of Hong Kong, (1988).
[18] Houston, B. P., Wolfendale, A. W., and Young, E. C. M., *J. Phys. G.: Nucl. Phys.*, 10(1984), L147.
[19] Avni, Y., Soltan, A., Tanabaum, H., and Zamorani, G., *Astrophys. J.*, 238 (1980), 800.
[20] Schmitt, J. H. M. M., *Astrophys. J.*, 293 (1985), 178.
[21] Marshall, H. L., *Astrophys. J.*, 299 (1985), 109.
[22] Cheng, F.-Z., Danese, L., De Zotti, G., and Franceschini, A., *M. N. R. A. S.*, 212 (1985), 857.
[23] Thompson, D. J. and Fichtel, C. E., *Astron. Astrophys.*, 109 (1982), 352.
[24] Hewitt, A. and Burbidge, G., *Astrophys. J. Suppl.*, 43 (1980), 57.
[25] Tananbaum, H., Avni, Y., Branduardi, G., Elvis, M., Fabbiano, G., Feigelson, E., Giacconi, R., Henry, J. P., Pye, J. P., Soltan, A., and Zamorani, G., *Astrophys. J.*, (*LettersS*), 234 (1979), L4.
[26] Kriss G. A. and Canizares, C. R., *Astrophys. J.*, 297 (1985), 177.
[27] Avni, Y. and Tananbaum, H., , *Astrophys. J.* (*Letters*), 262 (1982), L17.
[28] Riechert, G. A., Mason, K. O., Thorstensen, J. R., and Bowyer, S., *Astrophys. J.*, 260 (1982), 437.
[29] Weedman, D. W., *Ann. Rev. Astron. Astrophys.*, 15 (1977), 69.
[30] Weedman, D. W., *M. N. R. A. S.*, 184 (1987), 11P.
[31] Lau, M. M. and Young, E, . C. M., Proc. 20th Int. Cosmic Ray Conf., 1 (1987), 199.
[32] Jones, T. W., O'Dell, S. L. and Stein, W. A., *Astrophys. J.*, 188 (1974), 353.
[33] Lau, M. M., Young, E. C. M. and Yu, K. N., Proc. 3rd Asia Pacific Conf., in the press(1988).
[34] Hewitt, A. and Burbidge, G., *Astrophys. J. Suppl.*, 63 (1987), 1.
[35] Schwartz, D. A. and Ku, W. H-M., *Astrophys. J.*, 266 (1983), 459.
[36] Gioia, I. M. et al., *Astrophys. J.*, 283 (1984), 495.
[37] Burbidge, G. and Crowne, A. H., *Astrophys. J. Suppl.*, 40 (1979), 583.
[38] Worrall, D. M. et al., *Astrophys. J.*, 232 (1979), 683.
[39] Tananbaum, H. et al., *Ap. J.*, 305(1987), , 57.
[40] Owen, F. N., Helfand, D. J. and Spangler, S. R., *Astrophys. J.* (*Letters*), 250 (1981), L55.
[41] Condon, J. J., O'Dell, S. L., Puschell, J. J. and Stein, W. A., *Astrophys. J.*, 264 (1981), 624.
[42] Capps, R. W., Sitko, M. L. and Stein, W. A., *Astrophys. J.*, 255 (1982), 413.
[43] Baldwin, J. A. and Netzer, H., *Astrophys. J.*, 226 (1978), 1.
[44] Ku, W. H. M., Helfand, D. J. and Lucy, L. B. *Nature* 283 (1980)323.
[45] Kuhr, H., Witzel, A., Pauliny-Toth, I. I. K. and Nauber, U., *Astrn. Astrophy. Suppl.*, 45 (1981), 367.
[46] Impey, C. D. and Brand, P. W. J. L., *Nature*, 292 (1981), 814.
[47] Veron, M. P. and Veron, P., ESO Scientific Report No. 1, (1984).
[48] Mufson, S. L. et al., *Astrophys. J.*, 285 (1984), 571.

活动星系核的γ辐射

E.C.M.Young

K.N.Yu

(香港大学 应用科学系)

提　要

本文第1部份，描述从SAS-2卫星得到的能量大于100MeV的宇宙γ射线数据来证认有γ射线的活动星系核。11个类星体、3个BLLac天体和1个射电星系的γ射线辐射已得到证认。

本文第2部分描述活动星系核对河外γ射线背景辐射的影响。SAS-2的γ辐射数据，已被用来测定类星体和赛弗特星系的γ辐射绝对光度与光学绝对光度间的函数关系，并由此导出它们对河外γ射线背景辐射的贡献。我们指出，类星体($B<20$)、赛弗特星系(1型和1.5型)对35—100MeV能量范围的弥散γ射线背景辐射有相当大的贡献(59%)。由此我们得出河外γ射线背景辐射可能是由类星体和赛弗特星系这类活动星系产生的结论。

本文第3部份我们对3个有γ辐射的活动星系核综合其γ波段和其他波段的数据，以探索这些天体辐射的发射机制。这些综合的数据对发射机制给出严格的限制。我们指出，对这3个天体的数据，与同步自康普顿模型(SSC)的预计是一致的。